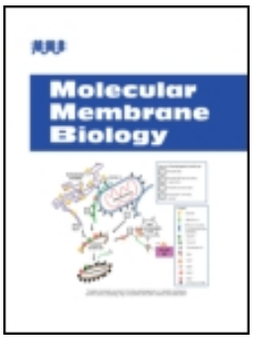

Molecular Membrane Biology

ISSN: 0968-7688 (Print) 1464-5203 (Online) Journal homepage: informahealthcare.com/journals/imbc20

Actin is not required for nanotubular protrusions of primary astrocytes grown on metal nano-lawn

Ulrike Gimsa, Aleš Iglič, Stefan Fiedler, Michael Zwanzig, Veronika Kralj-Iglič, Ludwig Jonas & Prof. Dr Jan Gimsa

To cite this article: Ulrike Gimsa, Aleš Iglič, Stefan Fiedler, Michael Zwanzig, Veronika Kralj-Iglič, Ludwig Jonas & Prof. Dr Jan Gimsa (2007) Actin is not required for nanotubular protrusions of primary astrocytes grown on metal nano-lawn, Molecular Membrane Biology, 24:3, 243-255, DOI: 10.1080/09687860601141730

To link to this article: https://doi.org/10.1080/09687860601141730

Published online: 09 Jul 2009.

Molecular Membrane Biology, May–June 2007; 24(3): 243–255

informa
healthcare

Actin is not required for nanotubular protrusions of primary astrocytes grown on metal nano-lawn

ULRIKE GIMSA[1], ALEŠ IGLIČ[2], STEFAN FIEDLER[3], MICHAEL ZWANZIG[3], VERONIKA KRALJ-IGLIČ[4], LUDWIG JONAS[5], & JAN GIMSA[6]

[1]*Research Institute for the Biology of Farm Animals, Research Unit Behavioural Physiology, Dummerstorf, Germany,* [2]*Laboratory of Physics, Faculty of Electrical Engineering, University of Ljubljana, Ljubljana, Slovenia,* [3]*Fraunhofer Institute for Reliability and Microintegration (IZM), Berlin, Germany,* [4]*Laboratory of Clinical Biophysics, Medical Faculty, University of Ljubljana,* [5]*Electron Microscopy Center, University of Rostock, Rostock, Germany, and* [6]*Chair of Biophysics, Faculty of Biology, University of Rostock, Rostock, Germany*

(Received 27 July 2006 and in revised form 26 October 2006)

Abstract

We used sub-micron metal rod decorated surfaces, 'nano-lawn' structures, as a substrate to study cell-to-cell and cell-to-surface interactions of primary murine astrocytes. These cells form thin membranous tubes with diameters of less than 100 nm and a length of several microns, which make contact to neighboring cells and the substrate during differentiation. While membrane protrusions grow on top of the nano-lawn pillars, nuclei sink to the bottom of the substrate. We observed gondola-like structures along those tubes, suggestive of their function as transport vehicles. Elements of the cytoskeleton such as actin fibers are commonly believed to be essential for triggering the onset and growth of tubular membrane protrusions. A rope-pulling mechanism along actin fibers has recently been proposed to account for the transport or exchange of cellular material between cells. We present evidence for a complementary mechanism that promotes growth and stabilization of the observed tubular protrusions of cell membranes. This mechanism does not require active involvement of actin fibers as the formation of membrane protrusions could not be prevented by suppressing polymerization of actin by latrunculin B. Also theoretically, actin fibers are not essential for the growing and stability of nanotubes since curvature-driven self-assembly of interacting anisotropic raft elements is sufficient for the spontaneous formation of thin nano-tubular membrane protrusions.

Keywords: *Nanostructures, primary cultures, tubules, gondolas, cytonemes, anisotropic membrane raft element*

Introduction

Research on cellular protrusions in the nm range is a rapidly expanding field. As cellular protrusions originate from different cell types and may not employ the same mechanisms, no common nomenclature has yet been established. Cellular protrusions are referred to as filopodia (Gerhardt et al. 2003), tunneling nanotubules (TNTs) (Rustom et al. 2004, Zhu et al. 2005), cytonemes (Morata & Basler 1999, Ramirez-Weber & Kornberg 1999), tethers (Cuvelier et al. 2005), or simply nanotubes (Önfelt et al. 2004). They appear to have a broad range of functions. Filopodia in living cells were first described by Gustafson and Wolpert (1961), who assumed that filopodia were extended to gather spatial information. Other functions ascribed to nanotubes extending from cells are the exchange of material or signalling molecules (Rustom et al. 2004, Zhu & Scott 2004, Watkins & Salter 2005). Nanotubes are even suspected of carrying cell organelles such as mitochondria (Spees et al. 2006). In addition, their formation is induced by intracellular bacteria such as *Listeria monocytogenes*, which use the tubes to travel from cell to cell (Merz & Higgs 2003, Robbins et al. 1999). It has been shown that cells of the immune system such as dendritic cells, B cells, T cells, NK cells, monocytes and neutrophils form nanotubes (Galkina et al. 2001, Gupta & DeFranco 2003, Önfelt et al. 2004, Watkins & Salter 2005). Nanotubes formed by B cells reach a length of up to 80 μm and are 200–400 nm in thickness. They often show a branched structure, with concentrated lipid raft-staining at the branching points. Otherwise, lipid raft structures are punctately

Correspondence: Prof. Dr Jan Gimsa, Chair of Biophysics, Faculty of Biology, University of Rostock, D-18057 Rostock, Germany. Tel: +49 381 498 6020. Fax: +49 381 498 6022. E-mail: jan.gimsa@uni-rostock.de

ISSN 0968-7688 print/ISSN 1464-5203 online
DOI: 10.1080/09687860601141730

distributed along the nanotube shafts and are especially to be found at the tip of the nanotube. Actin has also been found, similarly distributed along the shaft. However, the authors do not report a colocalization or whether they also found actin at the tips of the nanotubes (Gupta & DeFranco 2003). Besides these findings in fully functional, differentiated cells, nanotubes have also been observed in erythrocytes (Singer & Nicolson 1972, Sackmann 1994, Iglič et al. 2003).

Plasma membrane protrusions exhibit a specific protein and lipid composition differing from that of the planar region of the membrane (Weigmann et al. 1997). For example, the membrane protein prominin is preferentially localized in protrusions such as microvilli rather than in planar regions of the membrane, irrespective of the cell type (Weigmann et al. 1997, Corbeil et al. 2001). Therefore it has been suggested that accumulation of prominin (which exhibits no direct interactions with the actin-based cytoskeleton) in membrane protrusions has an important role in the generation and stabilization of the protrusions (Corbeil et al. 2001, Iglič et al. 2006). The redistribution of prominin after mild cholesterol depletion hints at the importance of cholesterol (Roper et al. 2000). Lipids are believed to play an important role as the interaction partners of prominin (Corbeil et al. 2001). Consequently, the state of the lipid phase is important in the formation of small prominin-lipid complexes and their coalescence into larger rafts after their curvature-induced accumulation in the membrane protrusions (Iglič et al. 2006).

Commonly, the cytoskeleton is considered to be the main determinant of membrane protrusions (Miyata et al. 1999 and references cited therein) and most of the observed cellular nanotubes indeed employ actin filaments. However, stable nanotubular structures may also develop in cell-free systems in the absence of actin (Mathivet et al. 1996, Karlsson et al. 2001, Karlsson et al. 2002, Kralj-Iglič et al. 2002, Roux et al. 2002, Roux et al. 2005). Cellular exocytosis has been modelled in protein-free liposomes and has been shown to involve nanotube formation by the membrane (Cans et al. 2003). Experimental and theoretical studies indicate their stabilization by accumulation and in-plane ordering of anisotropic raft elements (AREs) and anisotropic lipids (Kralj-Iglič et al. 2002, Kralj-Iglič et al. 2005). Tubular protrusions of phospholipid and erythrocyte membranes may also carry transport vesicles (gondolas) (Singer & Nicolson 1972, Iglič et al. 2003).

In this study, we focus on astrocytes. These cells comprise about 50% of the cells of the brain. They support neurons, both physically as a cellular matrix, and physiologically by providing a stable microenvironment and growth factors. Astrocytes form multicellular syncytia *in vivo* that ensure neuronal homeostasis by taking up excess neurotransmitters and buffering the ionic content of the extracellular medium (Hansson & Ronnback 1995, Walz 2000). They enwrap dendritic spines or whole synapses of neurons (Grosche et al. 1999, Ventura & Harris 1999). The physiological function of this intimate contact is probably to position signaling molecules directly to the sites of neurotransmission and to modulate neuronal communication (Hirrlinger et al. 2004). Astroglial membranes contain numerous neurotransmitter receptors and transporters and are thus equipped to sense and regulate formation, stability and efficacy of synapses (Ridet et al. 1997, Verkhratsky et al. 1998). Hirrlinger et al. (2004) showed motility of astrocytes *in situ*, i.e., in living brain slices. They showed extension of membrane tubes of <1 μm in diameter and 2–6 μm length. Their extension process lasts for 30–90 s. The majority of these filopodia stayed transiently elongated for 3–6 min while the minority stayed for longer than 15 min. Here, we demonstrate how primary murine astrocytes grow on sub-micron metal rod decorated surfaces, so-called 'nano-lawns'. Because of their special abilities of connecting cells in the brain, astrocytes make up an ideal model system for investigating the interaction of cells with nano-structured surfaces. Our main focus was on how the cells interact with the non-living material, how they form membrane protrusions, how cellular material is transported within these protrusions so that finally a confluent cell layer is formed. To this end we have used histological staining and scanning (SEM) as well as transmission electron microscopic imaging (TEM).

Materials and methods

Production of metal nano-lawns

Thin metal foils ($\sim$15 μm), decorated on one side with sub-micron metal rods ('nano-lawn') have been prepared according to the methods described by Schönenberger et al. (1997) using commercially available nucleopore-filters, i.e., chemically etched polycarbonate ion-track membranes (Millipore, 0.6 μm pores, Schwalbach, Germany) as template. Briefly, poly-carbonate filter membranes were coated by gold sputtering on one side to obtain a conductive metal layer. This layer was further enhanced galvanically by gold or platinum of up to approx. 10 μm thickness (Umicore Galvanotechnik, Germany). The polymer pores were filled by cathodic deposition of up to 3 μm. The polymer template was subsequently removed in boiling

dichloromethane (Figure 1A). The resulting metal foils were washed twice, then dried and cut. Substrate pieces of 3×2 mm^2 were sterilized in 70% aqueous ethanol prior to cell culture setup.

Properties of metal nano-lawn

Each metal pillar has a diameter of around 600 nm (Figure 1B and C). The density of the pillars on a typical template foil is approximately 3.5×10^{11} m^{-2}. Vertical pillars of platinum-nanolawn are around 1.6 μm long, and planar at the top (Figure 1B). The gold pillars are longer (around 2.6 μm) with tips of variously edged shapes, depending on the crystal structure at the tip (Figure 1C). Based on the technology of pore generation, the generated metal pillars follow a Poisson distribution.

Primary astrocyte cultures

Primary cortical astrocytes were isolated from neonatal mice as described earlier (Gimsa et al. 2004). Briefly, the frontal cortex was isolated from the brain, pools prepared and then mechanically dissociated through a nylon membrane. The cells were seeded onto poly-L-lysine (10 μg/ml in H_2O; Sigma-Aldrich, Taufkirchen, Germany) coated plastic dishes (2 brains per 6/24-well plate) and cultured in medium consisting of DMEM (Gibco BRL, Karlsruhe, Germany), plus 10% fetal bovine serum (Gibco), 100 U/ml penicillin/100 μg/ml streptomycin (Biochrom, Berlin, Germany), and 2.5 mM L-glutamine (Gibco). Astrocytes reached confluency after 10 days. They were detached by Accutase (PAA, Cölbe, Germany) treatment and seeded onto poly-L-lysin coated nanolawn structures. The

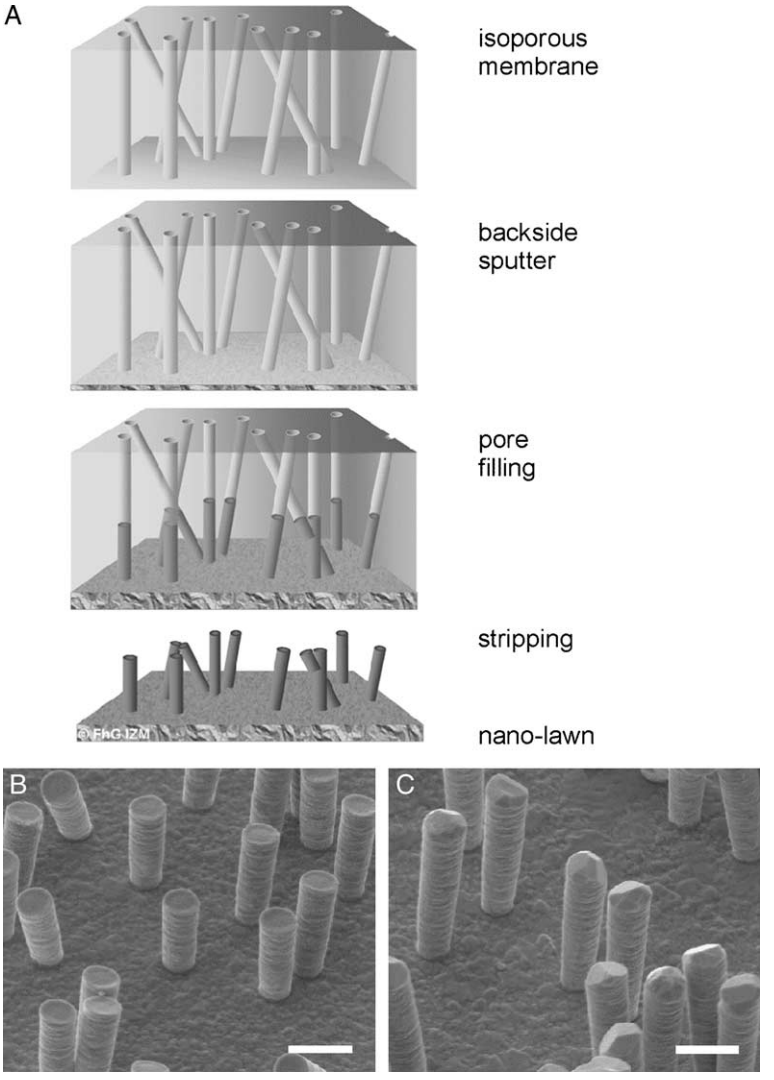

Figure 1. Sub-micron metal rod decorated surfaces; i.e., nanolawn. (A) Production of nano-lawn on isoporous track-etched polymer template. Polymer membranes are coated by gold-sputtering. This layer is enhanced in a platinum or gold plating bath. Polymer pores get filled by cathodic deposition. Polymer template gets removed. Depending on metal plating conditions, multicrystalline pillars with different grain size can be produced. (B) Platinum nano-lawn. (C) Gold nano-lawn. Scale bars of SEM images in B and C represent 1 μm.

cells were fixed for 1 h in 4% glutaraldehyde in PBS for electron microscopical examination after 24 h or 72 h of culture on nano-lawns. Cells were fixed after staining (see below) for 10 min in 2% formaldehyde in PBS for histological examination following 72 h of culture on nano-lawns.

Latrunculin B treatment

For latrunculin B treatment, cells were seeded as before onto nano-lawns and incubated in medium containing 5 μM or 10 μM latrunculin B (Calbiochem/Merck, Darmstadt, Germany). The cells were fixed after 1 h or 24 h. In addition, the effect of actin depolymerization was checked by exchanging control medium by medium containing latrunculin B, following culturing periods of 1 h or 23 h. These cultures were fixed 1 h later.

CFSE and propidium iodide staining

Cells on nano-lawns and microscopic slides were labeled with CFSE (10 μM 5(6)-carboxyfluorescein diacetate succinimidyl ester, mixed isomers; Molecular Probes/MoBiTec, Göttingen, Germany) for 7 min and then washed. Propidium iodide staining was performed on other cell samples by incubating the cells for 5 min with 10 μM propidium iodide, followed by washing.

SEM and TEM imaging

Samples for SEM were washed, fixed in 4% glutaraldehyde in PBS, washed again, postfixed in 1% osmium tetroxide, dehydrated in acetone, and subjected to critical-point drying (EMITECH K850, Ashford, Kent, UK). The samples were sputtered with colloidal gold using a Sputter Coater (BALTEC SCD 004, Schalksmühle, Germany) before examination in the SEM (DSM 960 A, Zeiss, Oberkochen, Germany). Samples for TEM were fixed in 4% glutaraldehyde in PBS, washed in PBS, postfixed in 1% osmium tetroxide, dehydrated in a graded series of ethanolic solutions, and embedded in Araldite (Fluka, Buchs, Switzerland). Ultrathin sections were prepared with a diamond knife using an Ultracut ultramicrotome (Leica, Bensheim, Germany), mounted on copper grids, stained with uranylacetate and lead citrate, and examined with a TEM (EM 902 A, Zeiss, Oberkochen, Germany).

Results and discussion

Cell status on nano-lawns

We used platinum or gold nano-lawns to grow primary murine astrocytes. Indeed, these unusual culture substrates were equally accepted without adverse effects. Astrocyte morphology was very similar on glass slides (Figure 2A) and nano-lawns (Figure 2C, E). Cell death was negligible according to propidium iodide staining after 72h of culture (Figure 2B, D, F). This is in line with previous observations of astrocytes growing on silicon pillar arrays (Turner et al. 2000).

Our astrocytes formed contacts to the metal pillars within minutes (Figure 3A and B). Indeed, the formation of nanotubes could have been much more rapid than that, as 10 min was the shortest time interval we examined. Recently, the formation of astrocyte filopodia-like processes has been observed within seconds (Hirrlinger et al. 2004). Moreover, these filopodia retract again within minutes, a process which we could not observe since our cultures had been fixed before analysis. In our cultures, astrocytes extended nanotubes to neighboring metal pillars and from there to further pillars while maintaining contact to pillars that had been reached before (Figure 3C). The angle between an attached nanotube and the continuative tube is in the 90–180° range. Nanotubes may branch into 2 continuing nanotubes (Figure 3C). Similar to a culture on glass slides (Figure 2A), astrocytes display various cell shapes (Figure 3F). However, when observed in detail, the nanotubes appeared straightened between two attachment points on metal pillars while their correspondent structures, grown on poly-L-lysin coated glass surfaces, (Figure 3D) displayed serpentine shapes. Such a straightened appearance has been described by Önfelt et al. (2004). They found a branched nanotube connecting three B cells. When one connection broke, the remaining nanotube contracted, so connecting two cells but still keeping a straightened appearance. They hypothesized that this contraction was possible due to the nanotube composition of fluid membrane that can flow easily between the nanotubes and the cell surface. The nanotubes extended over several μm at a diameter below 100 nm (Figure 3E) but sometimes developed into very long tubes (>100 μm) at a higher diameter (still <1 μm) (Figure 3F). We assumed from our observations that astrocytes aimed at growing to confluency by making contact to cells further away (Figure 3G). Apparently, they first extended nanotubular protrusions to bridge the gap in between cells before closing it by cellular material traveling along the nanotubes (Figure 3H). The alternative explanation, namely that the cells in Figure 3H disengaged from each other while leaving behind nanotubular connections, is unlikely as we observed a strong decrease of these gaps of the cells with time. Depending on the number of cells seeded in, confluency could be reached within 24 h.

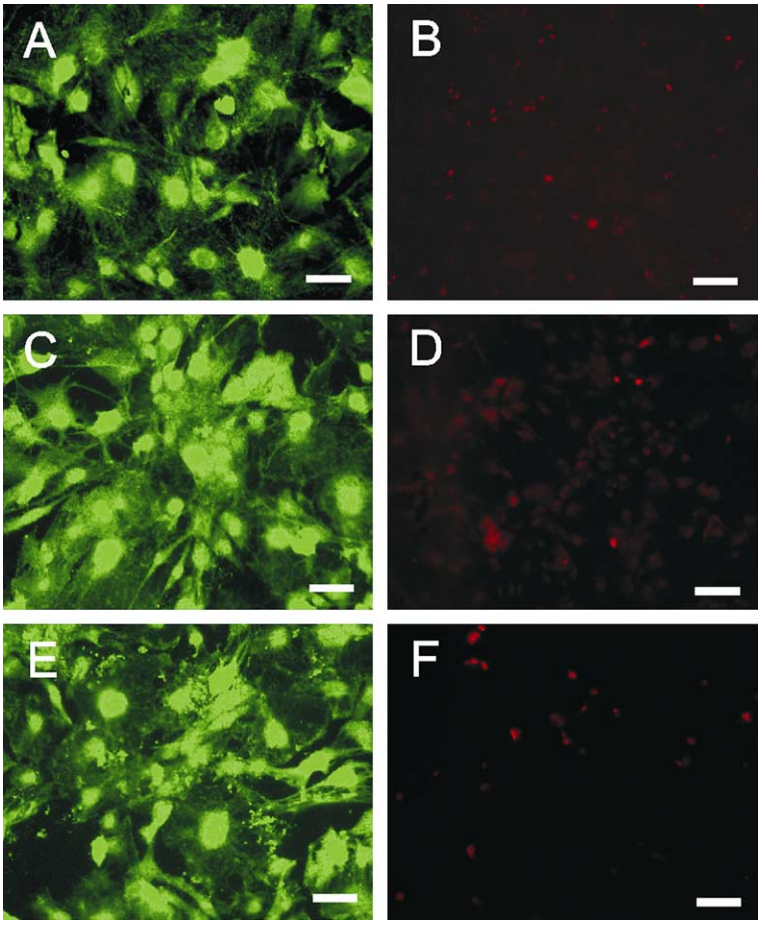

Figure 2. Primary murine astrocytes after 72 h on poly-L-lysin coated glass slides (A, B), platinum (C, D) or gold (E, F) nanolawns. Astrocytes were stained intracellularly with CFSE (A, C and E) or propidium iodide (B, D and F) revealing uncompromised growth and negligible cell death on nano-lawns. Scale bars in A, C and E represent 50 μm; scale bars in B, D and F represent 100 μm. This Figure is reproduced in color in *Molecular Membrane Biology* online.

Apparently, the material necessary to prolong the tubes was transported along the nanotubes in gondola-like structures (Figure 3H–J). This notion is supported by our observation of gondola-like structures as early as 10 min of culture when nanotubular extensions start the process of monolayer formation on nanolawns from cells which are spherical and singularized at the moment of seeding (Figure 3B). Membrane nanotubes connecting macrophages have been reported to carry 'bulges' travelling along the nanotubes (Önfelt et al. 2004). The nanotubes indeed transported cellular material as the authors showed that lipids from two cells mixed. Thus, they assumed that the nanotubes also provide a mechanism for the intercellular transfer of cell surface proteins (Önfelt et al. 2004). In addition to nanotube formation from actin-driven protrusions described by Rustom et al. (2004), they found nanotube formation between cells that were previously connected via an immunological synapse as cells separated (Önfelt et al. 2004).

Cell bodies and nuclei were found sagged in between metal pillars (Figure 4A) while nanotubular protrusions seem to be restricted to the upper parts of the pillars (Figure 4B). When observed from an angle, it became clear that this also applied to the peripheral membrane surfaces (Figure 4B and C). The backside of the cell monolayer showed clear imprints of the nanotubes (Figure 4C). The contact these cells formed to the pillars were close, i.e., in the nm range (Figure 5) resembling those seen between astrocytic processes and neurons (Duan et al. 2004). Hirrlinger et al. (2004) described that the astrocytic somata stayed stationary. This corresponds to our finding that somata with nuclei are found in between pillars where they could not easily move (Figure 4A).

Actin involvement – common knowledge on nanotubes and our findings

Actin fibers have been suggested to be responsible for nanotubular transport (Rustom et al. 2004). We examined whether this mechanism applied to our

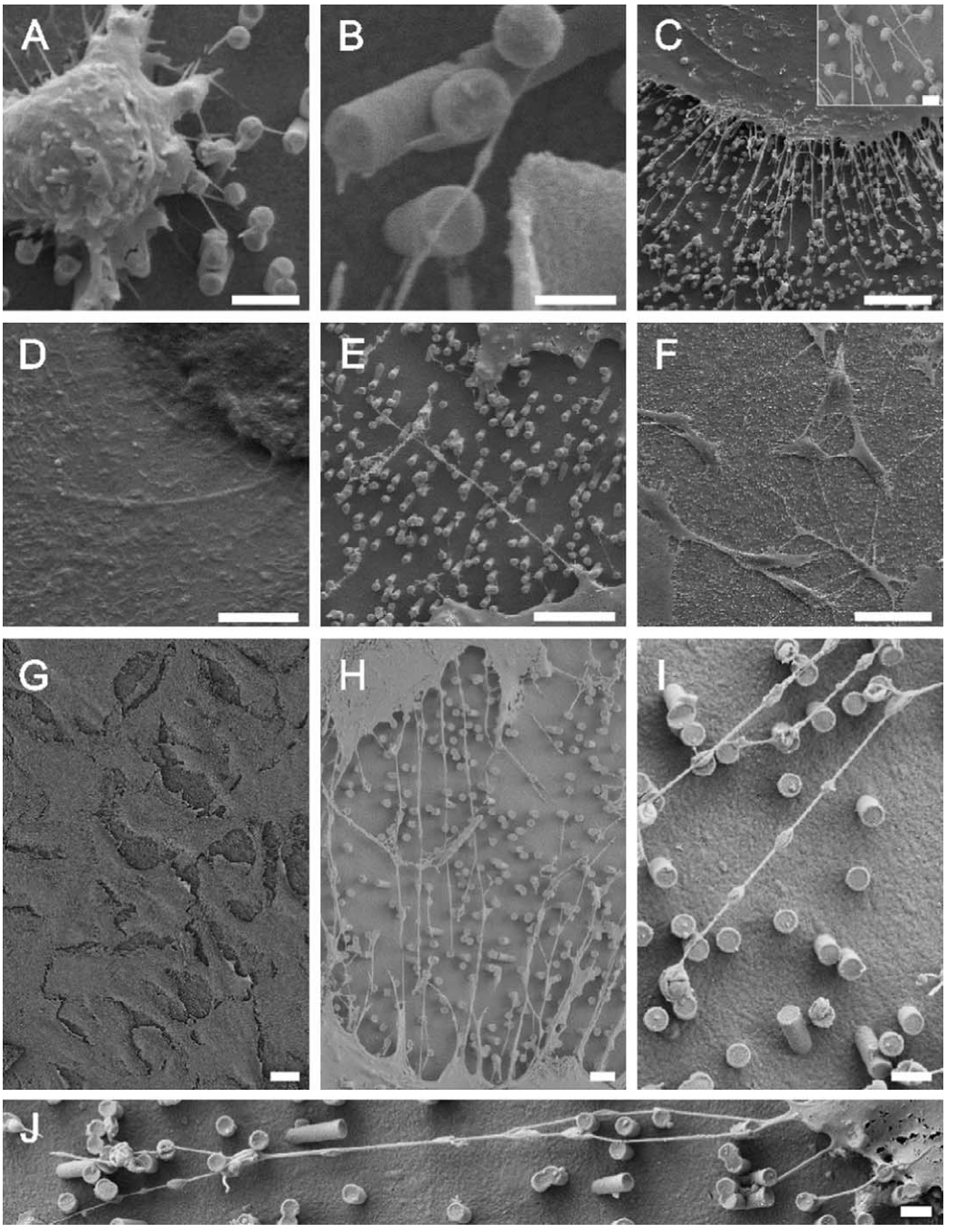

Figure 3. Astrocytes growing on nano-lawns (SEM images). Astrocytes make contact to metal pillars via nanotubular membrane protrusions within 10 min (A, B). They extend nanotubes to distant metal pillars via neighboring pillars while maintaining contact to pillars that were reached before (C). Nanotubes appear straightened in between two attachment points on metal pillars while their correspondent structures grown on poly-L-lysin coated glass surfaces are randomly coiled (D). Nanotubes may extend over several μm at a diameter of about 100 nm (E) but may develop into very long tubes ($>$100 μm) at a higher diameter which is still $<$1 μm (F). Astrocytes grow to confluency by making contact to cells further away (G). It can be assumed that astrocytes first bridge the gaps between cells by nanotubular protrusions before closing them with more cellular material (H). Apparently, the material necessary to prolong these nanotubes was transported along the nanotubes in gondola-like structures (H–J) which have been observed as early as 10 min after start of culture (B). Scale bars in A, B, C, D, E, F, G, H and I represent 2, 0.8, 10 (insert: 1), 200, 8, 20, 20, 2, 1 and 1 μm, respectively. Nanostructures were gold (A, B, C, E) or platinum (F, G, H, I, J).

system, too. To this end, we treated the cells with latrunculin B which is known to both prevent polymerization of actin and to depolymerize actin filaments (Rustom et al. 2004). Surprisingly, the formation of nanotubes was not affected by 5 (Figure 6A) and 10 μM (Figure 6B) latrunculin B 1 h after cell seeding. The same was true for cells cultured for 24 h in the presence of latrunculin B

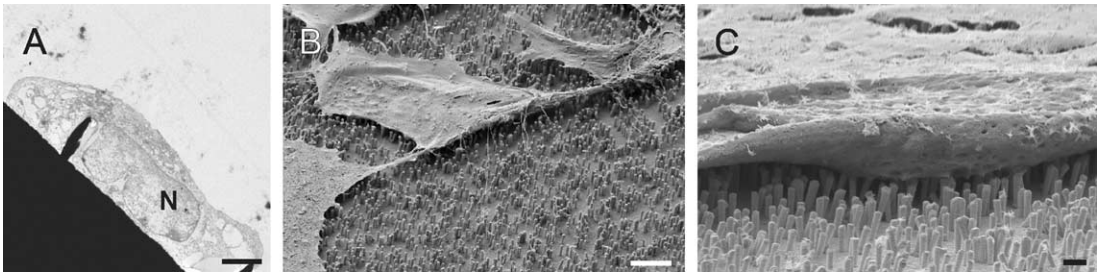

Figure 4. TEM images show that cell bodies and nuclei (marked by 'N') were found in between metal pillars (A) while nanotubular protrusions as well as peripheral membrane parts seem to be restricted to the upper parts of the pillars as revealed by SEM images taken at an angle of 45° (B) or 60° (C). The flipped-over cell monolayer in C revealed that it rested on tips of pillars (note imprints of pillars). Scale bars in A, B and C represent 2, 10 and 2 μm, respectively. Nanostructures were gold.

(Figure 6C, D). Furthermore, the stability of nanotubes was not compromised by treatment with 5 (Figure 6E) and 10 μM (Figure 6F) latrunculin B compared to control cells 2 h after cell seeding. In the latter experiments, latrunculin B was added for 1 h after the cells had been allowed to settle for 1 h (Figure 6E and F). However, it was apparent that latrunculin B was active, as we found an overall diminished stability of the cells at 10 μM latrunculin B as even the membranous parts of the cells seemed to sink in between the metal pillars (Figure 6F). These findings suggest that actin fibers do not play a major role in nanotube formation or stability. This corresponds to a hypothesis of Önfelt et al. (2004) that nanotubes are constructed from fluid membrane. It is also in line with findings from Karlsson et al. (2001, 2002) and our laboratories (Kralj-Iglič et al. 2002) that nanotubes and gondolas can be formed in pure phospholipid systems.

Nanotubes branching into nets

Interestingly, we found branched nanotubes forming nets of tubes expanding between cells (Figure 7A and B). These branched nanotube networks could indicate a special growth pattern or a pattern of what cells leave behind when they retreat as they do when they round up and die. Indeed, we never found them in very fresh cultures (e.g., 2 h) but in cultures >24 h in which we also found rounded, most likely apoptotic cells 'spun' in nets (Figure 7C). Thus, we assume it more likely that the branched tubular networks are leftovers of highly interconnected cells which have undergone apoptosis.

Since the nanotubes formed under the influence of latrunculin B did not display regular net branching as seen in Figure 7, we assume they are not traces left behind by moving or dying cells. Another supporting argument for our view that actin (Miyata et al. 1999) or a permanent pulling force (Sun et al. 2005) are not essential for the formation and stability of nanotubes comes from pure phospholipid systems where stable nanotubes have been observed (Iglič et al. 2003, Kralj-Iglič et al. 2002, Mathivet et al. 1996). Nevertheless, the fact that actin is not necessary for the formation of nanotubes does not preclude it having some supportive role in fiber formation inside the tubes (Corbeil et al. 2001, Iglič et al. 2006). Astrocytes may utilize an actin-independent cytoskeleton formed by glial fibrillary acidic protein (GFAP), which is a unique marker of these cells. Astrocytes are coupled via thin processes. Apparently, these processes contain

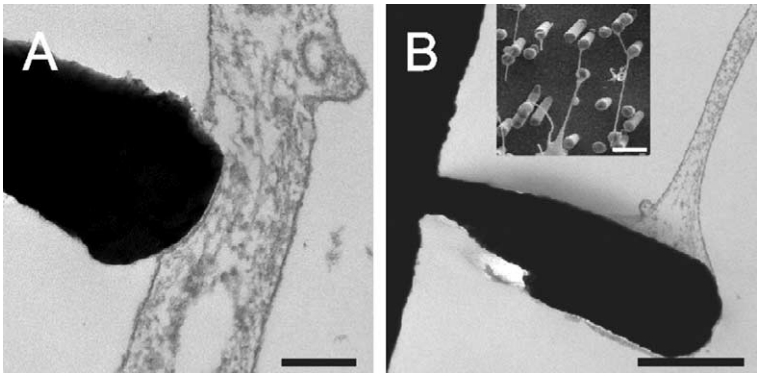

Figure 5. TEM images show that astrocytes make very close contact to the pillars with a distance in the nm range (A and B). SEM image (insert in B) shows that nanotubes end on pillars in a bulb-like contact. Scale bars in A and B represent 200 nm and 1 μm (insert: 2 μm), respectively. Nanostructures were gold.

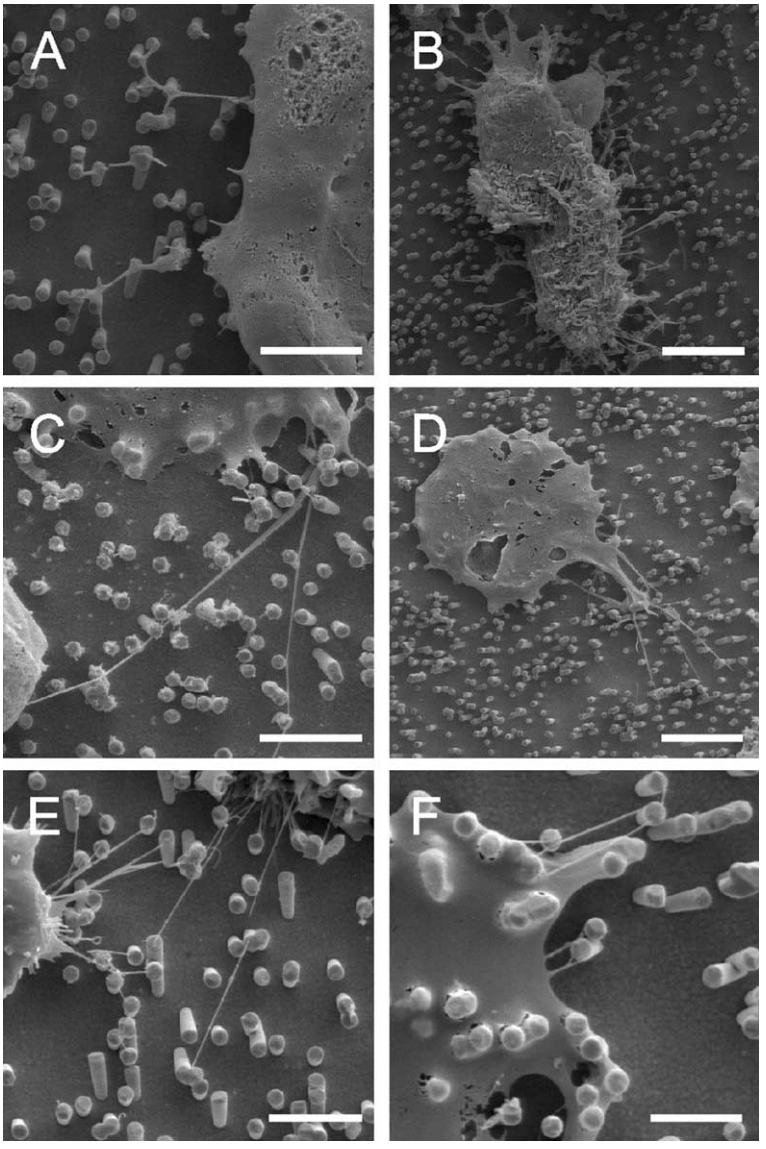

Figure 6. The formation and stability of nanotubes is not affected by latrunculin B. Astrocytes were cultured in the presence of latrunculin B for 1 h (A, B) or 24 h (C, D): 5 μM (A, C); 10 μM (B, D). To test the stability of nanotubes in the absence of actin, astrocytes were seeded onto nano-lawns for 1 h before addition of 5 (E) and 10 μM (F) latrunculin B for another hour. Scale bars in A–F represent 5, 10, 5, 10, 4, and 3 μm, respectively. Nanostructures were gold.

GFAP, suggesting that GFAP could be a structural component in process formation (Duval et al. 2002).

Possible mechanism of growing and stability of nanotubes and thin membrane protrusions

It is generally accepted (Derenyi et al. 2002, Kralj-Iglič et al. 2005, Miao et al. 1991, Tsafrir et al. 2003) that the standard theory of isotropic membrane elasticity (Deuling & Helfrich 1976, Sackmann 1994) cannot explain growing and stability of nanotubular membrane protrusions. Therefore, we suggest a new mechanism that may theoretically explain the observed formation of nanotubes by astrocytes in the absence of actin fibers. The proposed mechanism is based on the energetically favorable self-assembly of interacting AREs into larger raft domains (Hägerstrand et al. 2006) in the form of nanotubes (Corbeil et al. 2001). These AREs are defined as very small flexible membrane domains composed of a number of membrane components (Hägerstrand et al. 2006 and references therein).

Thin biological membranes can be described as two-dimensional surfaces characterized by two principal curvatures C_1 and C_2. Single raft elements are generally anisotropic with respect to the curvature of their normal cuts and can be considered as thin flexible shells with various equilibrium shapes. These elements are neither flat nor

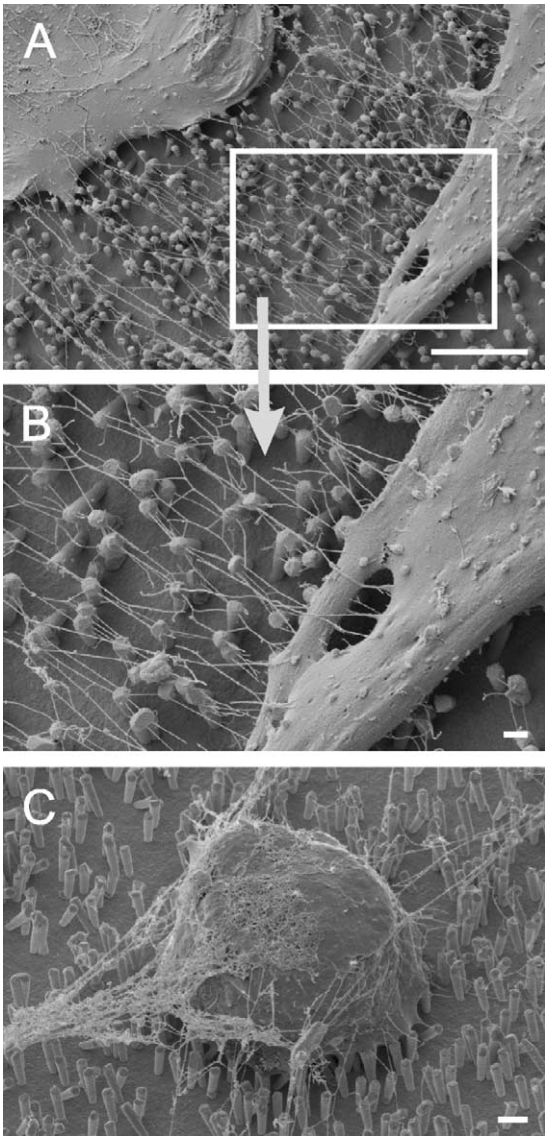

Figure 7. Branched nanotubes forming nets of tubes expanding between cells at different magnifications (A and B). In the same culture, globular, contracted cell bodies covered with a net-like structure (B) were found suggesting that branched nanotubes might not occur when cells colonize nanostructures but rather reflect leftovers of cells having retreated from nanostructures before undergoing apoptosis. Scale bars in A, B and C represent 10, 1 and 2 μm, respectively. Nanostructures were gold.

spherical (Figure 8). The shape of a single ARE can be characterized by two intrinsic, spontaneous principal curvatures C_{1m} and C_{2m} with $C_{1m} \neq C_{2m}$ (Figure 8) and by its orientation in the principal systems of the actual local membrane curvature tensor (Figure 9).

For $C_{1m} = C_{2m}$, the raft element would be isotropic. Anisotropy and flexibility allow the raft elements to adapt their shapes and orientations to the actual membrane curvature which in turn is influenced by the AREs. Different orientations with respect to the local principal axes of the membrane

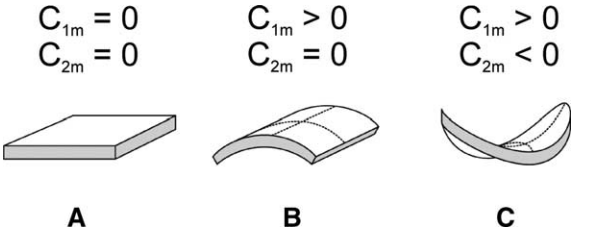

Figure 8. Schematic figure of the favorable shapes of flexible membrane raft elements with different intrinsic (spontaneous) principal curvatures C_{1m} and C_{2m}. (A) isotropic shape for $C_{1m} = C_{2m} = 0$; (B) anisotropic shape for $C_{1m} > 0$ and $C_{2m} = 0$; and (C) anisotropic shape for $C_{1m} > 0$ and $C_{2m} < 0$.

(described by the angle ω) yield different energies of the ARE (Iglič et al. 2005):

$$E(\omega) = \frac{\xi}{2}(H - H_m)^2 + \frac{\xi}{2} \times (D^2 - 2DD_m\cos(2\omega) + D_m^2), \quad (1)$$

with $H = (C_1 + C_2)/2$ being the mean curvature, $D = |C_1 - C_2|/2$ the curvature deviator, $D_m = |C_{1m} - C_{2m}|/2$ the intrinsic curvature deviator, $H_m = (C_{1m} + C_{2m})/2$ the intrinsic mean curvature and ξ a constant. It can be expected that an ARE spends more time in energetically favorable orientational states.

The partition function (see also Hill 1986) of a single ARE can be written in the form:

$$Q = \frac{1}{\omega_0}\int_0^{2\pi} \exp\left(-\frac{E(\omega)}{kT}\right) d\omega, \quad (2)$$

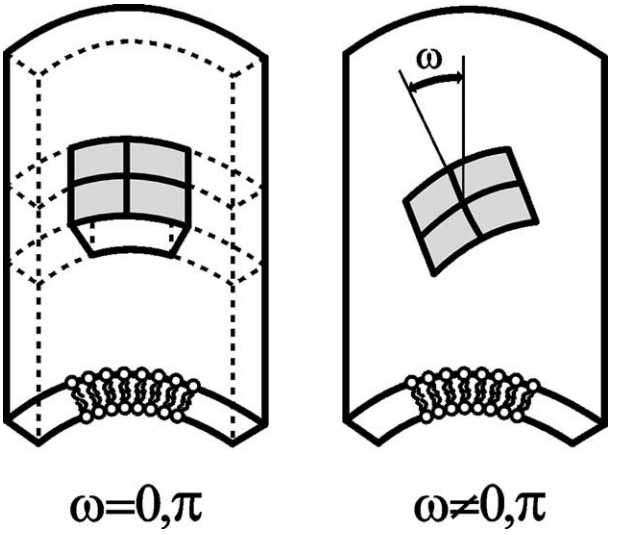

Figure 9. Schematic figure of different orientation of an anisotropic raft element (ARE) with intrinsic principal curvatures $C_{1m} > 0$ and $C_{2m} = 0$ in a barrel-section shaped membrane section with principal curvatures $C_1 > 0$ and $C_2 = 0$. Left: energetically favorable orientation. Right: a flexible ARE will be bent in the curvature field of the membrane – unfavorable orientation.

where ω_0, k, and T stand for an arbitrary angle quantum, the Boltzmann constant, and the absolute temperature, respectively. The free energy of a single ARE $= -kT \ln Q$ is:

$$f = \frac{\xi}{2}(H - H_m)^2 + \frac{\xi}{2}(D^2 + D_m^2) - kT\ln\left(I_0\left(\frac{\xi D_m D}{kT}\right)\right), \quad (3)$$

where I_0 is the modified Bessel function.

An ARE may interact with neighboring raft elements forming aggregates. We denote the corresponding interaction energy per monomeric ARE in an aggregate composed of i raft elements as $\chi(i)$ and assume that $\chi(i)$ depends on the size of the aggregate. Please note that i is the aggregation number throughout the manuscript. Hence, the mean energy per ARE in a cylindrical aggregate of i raft elements can be written as $\mu_i = f_c - \chi(i)$, where $f_c = f(H = D)$ and $\chi(i) > 0$. Since AREs in flat regions exhibit a high mean energy of $\tilde{\mu}_i = f_p$, with $f_p = f(H = D = 0)$, we assume that their concentration is always below the critical aggregation concentration (CAC) (for definition see Israelachvili 1997) in the planar regions of the membrane (with $H = D = 0$). Therefore, AREs will not form two-dimensional aggregates in the flat membrane regions. The mole-fraction concentration of the AREs in the flat membrane regions is $\tilde{x}_1 = \tilde{N}_1/M$, with $\tilde{N}_1$ being the number of monomeric AREs in flat regions and M the number of (lattice) sites in the whole system. The size distribution of cylindrical aggregates on the concentration scale is $x_i = iN_i/M$, where N_i denotes the number of cylindrical aggregates with aggregation number i, i.e., the number of tubular membrane protrusions (N_i). The concentrations $\tilde{x}_1$ and x_i should fulfill the conservation conditions for the total number of AREs in the membrane: $\tilde{x}_1 + \sum_{i=1}^{\infty} x_i = N/M$. The free energy of all AREs in the membrane is composed of the energies of the raft elements and all aggregates as well as the mixing entropy of the raft elements and all aggregates. Raft aggregates of the same size are treated as equal and indistinguishable. Using the Lagrange method, minimization of the function:

$$f = M\left[\tilde{x}_1\,\tilde{\mu}_1 + kT\,\tilde{x}_1(\ln\tilde{x}_1 - 1)\right] + M \times \sum_{i=1}^{\infty}\left[x_i\mu_i + kT\frac{x_i}{i}\left(\ln\frac{x_i}{i} - 1\right)\right] - \mu M\left(\tilde{x} + \sum_{i=1}^{\infty} x_i\right), \quad (4)$$

with respect to $\tilde{x}_1$ and x_i, leads to the equilibrium distributions:

$$\tilde{x}_1 = \exp\left(-\frac{f_p - \mu}{kT}\right), \quad (5)$$

$$x_i = i\exp\left(-\frac{i}{kT}[f_c - \chi - \mu]\right), \quad (6)$$

where μ is the Lagrange parameter. For simplicity, we assumed $\chi(i)$ to be constant. The quantity μ can be derived from Equation (5) and inserted in Equation (6) to get:

$$x_i = i\left[\tilde{x}_1 .\exp\left(\frac{f_p + \chi - f_c}{kT}\right)\right]^i. \quad (7)$$

Since x_i can not exceed unity, from Equation (7) follows that $\tilde{x}_1$ can not exceed $\exp((f_c - f_p - \chi)/kT)$. The maximal concentration of AREs in the flat membrane parts $\tilde{x}_1$ therefore is:

$$\tilde{x}_c \approx \exp\left(\frac{\Delta f - \chi}{kT}\right), \quad (8)$$

where $\Delta f = f_c - f_p$ is the difference between the energies of a single ARE in a cylindrical protrusion and in the flat membrane region. The concentration $\tilde{x}_c$ is the CAC. In the case of cylindrical aggregates where $H = D = 1/2r$ from Equation (3) follows:

$$\Delta f = \xi H(H - H_m) - kT\ln[I_0(\xi D_m D/kT)] \quad (9)$$

For $1/2r < H_m$ the value of Δf is always negative. For $\tilde{x}_1$ above $\tilde{x}_c$, the self-assembly of very long cylindrical aggregates is promoted (Figure 10).

AREs undergo orientational ordering on the tubular aggregates, thereby forming regions of higher order within the membrane. These aggregates

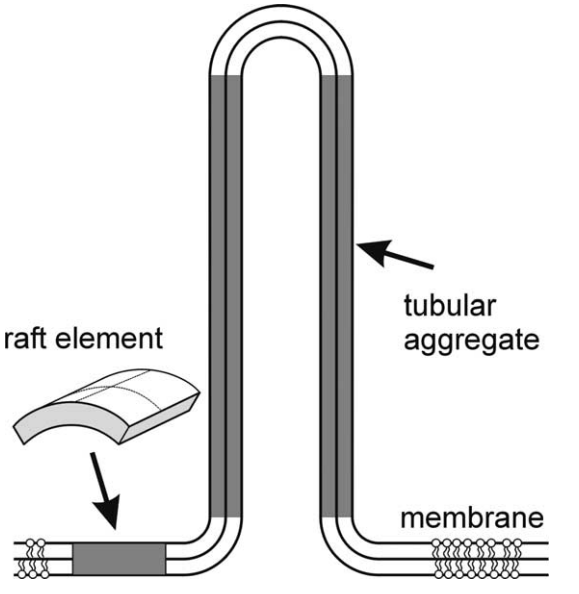

Figure 10. Schematic figure for the energetically favorable self-assembly of cylindrical aggregates by interacting anisotropic raft elements (AREs with $C_{1m} > 0$ and $C_{2m} = 0$).

are consistently related to the stable tubular shape with a particular equilibrium radius (Figure 10). However, the concentration of monomeric AREs in the tubular part is higher than in the flat parts already when the monomer concentration in the flat parts is below the critical concentration ($\chi_1 >> \tilde{x}_1$ also for $\tilde{x}_1 < \tilde{x}_c$) indicating that AREs may play an important role in generation and stabilization of nanotubes even below the CAC. Equations (8) and (9) show that the longitudinal growth of nanotubes is promoted by the energy difference Δf as well as by the strength of the direct interactions between the AREs χ. The critical concentration $\tilde{x}_c$ strongly decreases with increasing D_m.

In the above model, no actin fibers generating a pulling or pushing force are necessary to explain the growth and stability of nanotubes. Such a force is required within the classical theory of isotropic membrane elasticity (Derenyi et al. 2002, Kralj-Iglič et al. 2005, Miao et al. 1991, Tsafrir et al. 2003). However, in systems where tubes are indeed formed by a pulling or pushing force (e.g., in systems that involve motor proteins on cytoskeletal filaments), the proposed mechanism can contribute to the stabilization of nanotubular membrane protrusions.

Within the above theory, the critical membrane concentration of AREs required for the spontaneous formation of nanotubes strongly decreases with an increasing intrinsic curvature deviator $D_m = |(C_{1m} - C_{2m})|/2$ of the AREs. This suggests that the growth of nanotubular membrane protrusions is favored by a high concentration of AREs.

Gondolas

To the best of our knowledge, no consistent theoretical explanation exists for the formation of gondolas. Nevertheless, we believe that the initiation of gondola formation must be based on similar physical mechanisms like membrane budding (Iglič & Hägerstrand 1999; Hägerstrand et al. 2006). In contrast to the latter process, in gondolas, the connection to the parent membrane from where they originate is not disrupted. Once the gondola is formed, its movement along the nanotube requires no additional bending energy. Nevertheless, an energy delivering process is required in order for the gondola to travel along the nanotube. Theoretically, gondola movement may be driven by the difference in chemical potential between the two compartments connected by the nanotube (Karlsson et al. 2001), i.e., the transport of the molecules packed inside the gondola degrades the potential difference. The final event may be the fusion with a target membrane (Iglič et al. 2003, Jahn et al. 2003). In this process, those molecules of the gondola's membrane which originate from the parental, nearly flat membrane distribute again in the almost flat (target) membrane. This may be energetically favorable and therefore a part of a driving mechanism to facilitate the fusion of the gondola with the target membrane. Also note that prior to the fusion of the gondola with the target membrane, no neck formation is needed when a gondola arrives at its 'final destination' (contrary to the case of a free transport vesicle (Jahn et al. 2003)) since the neck is already a part of the nanotube connected to the membrane of the destination cell. Therefore, gondola transport may be energetically better than free vesicle transport. Recent studies indicate that vesicular transport between cell organelles over longer distances is not random and takes place between specific surface regions of cell organelles (Sprong et al. 2001; Iglič et al. 2004). Such organized transport has been described for material in vesicles (Rustom et al. 2004) and as the exchange of membrane constituents via nanotubes (Watkins & Salter 2005).

Alternatively to the fusion with a membrane of small curvature, gondola material might be used for elongation of nanotubes to facilitate bridging of long distances to pillars of the nano-lawn or between cells. The energetic balance of this process will depend on the curvature of the terminal tip. It might be bulb-shaped, as described for the outgoing/afferent protrusions from the nose sensory cells of pikes (Buchner et al. 1987). Very similar shapes can be seen when nanotubes make contact to pillars (insert into Figure 5B).

Conclusions and outlook

A number of recent studies indicate that nanotubes are common and important in cell structure and function (Robbins et al. 1999, Galkina et al. 2001, Gupta & DeFranco 2003, Merz & Higgs 2003, Önfelt et al. 2004, Rustom et al. 2004, Zhu & Scott 2004, Watkins & Salter 2005, Spees et al. 2006). Nanotubes may transport cellular compounds between cells or cell organelles either directly or direct the transport of carrier vesicles, such as gondolas (Karlsson et al. 2001, Iglič et al. 2003, Rustom et al. 2004).

The predictions of our new theory on nanotube formation are in line with the experimental findings. Our description upgrades the fluid mosaic model of cellular membranes by the introduction of AREs (Singer & Nicolson 1972). Even though a theoretical description of gondola formation and traveling is not yet available, our experimental evidence suggests that nanotube-directed transport of carrier vesicles is

not restricted to interactions between cells but also occurs in cells grown on non-cellular substrates. For this growth, the surface geometry is at least as important as surface chemistry as a determinant for the quality of cell-surface interaction in nanostructured systems. This is suggested by the similarity of cell behavior on platinum and gold structures. Cell-matrix interactions in systems with nano-pillars made of silicon (Turner et al. 2000) very much resemble those on our gold and platinum nano-lawns.

The extremely close contact of astrocytes (and perhaps other cells) to nanostructures as growth substrates offers chances for (i) applications for contacting cells electrically; (ii) forming model tissues; (iii) contact formation in microsystems technology. The ability of astrocytes to grow on nano-lawn might be of particular relevance for scaffolding technologies in new neurosurgical therapeutic approaches, directing the growth pattern of astrocytes on artificial substrates to pave the way for neuronal sprouting (Bakshi et al. 2004, Ellis-Behnke et al. 2006).

Acknowledgements

This study has been supported by grants 01 ZZ 0108 from the Bundesministerium für Bildung und Forschung (Federal Ministry for Education and Research) and the Hertie Foundation (1.01.1/03/014) to U.G. and StSch 2002 0418A from the Bundesamt für Strahlenschutz (Federal Office for Radiation Protection) to J.G. S.F. and M.Z. have been financed by IZM intramural funding. The authors thank the staff of the electron microscopy center at the University of Rostock's Medical Faculty for outstanding technical support. C. Voigt is acknowledged for excellent technical assistance. The authors are grateful to B. Babnik for help with preparation of the figures and to R. Sleigh for help with the manuscript. The German Academic Exchange Service (DAAD) fellowship supporting the stay of A. I. at the University of Rostock is gratefully acknowledged.

References

Bakshi A, Fisher O, Dagci T, Himes BT, Fischer I, Lowman A. 2004. Mechanically engineered hydrogel scaffolds for axonal growth and angiogenesis after transplantation in spinal cord injury. J Neurosurg Spine 1:322–329.

Buchner K, Seitz-Tutter D, Schonitzer K, Weiss DG. 1987. A quantitative study of anterograde and retrograde axonal transport of exogenous proteins in olfactory nerve C-fibers. Neuroscience 22:697–707.

Cans AS, Wittenberg N, Karlsson R, Sombers L, Karlsson M, Orwar O, Ewing A. 2003. Artificial cells: unique insights into exocytosis using liposomes and lipid nanotubes. Proc Natl Acad Sci USA 100:400–404.

Corbeil D, Roper K, Fargeas CA, Joester A, Huttner WB. 2001. Prominin: a story of cholesterol, plasma membrane protrusions and human pathology. Traffic 2:82–91.

Cuvelier D, Derenyi I, Bassereau P, Nassoy P. 2005. Coalescence of membrane tethers: experiments, theory, and applications. Biophys J 88:2714–2726.

Derenyi I, Jülicher F, Prost J. 2002. Formation and interaction of membrane tubes. Phys Rev Letters 88:238101-01-238101/04.

Deuling HJ, Helfrich W. 1976. The curvature elasticity of fluid membranes: a catalogue of vesicle shapes. J Phys (France) 37:1335–1345.

Duan L, Yuan H, Su CJ, Liu YY, Rao ZR. 2004. Ultrastructure of junction areas between neurons and astrocytes in rat supraoptic nuclei. World J Gastroenterol 10:117–121.

Duval N, Gomes D, Calaora V, Calabrese A, Meda P, Bruzzone R. 2002. Cell coupling and Cx43 expression in embryonic mouse neural progenitor cells. J Cell Sci 115:3241–3251.

Ellis-Behnke RG, Liang YX, You SW, Tay DK, Zhang S, So KF, Schneider GE. 2006. Nano neuro knitting: peptide nanofiber scaffold for brain repair and axon regeneration with functional return of vision. Proc Natl Acad Sci USA 103:5054–5059.

Galkina SI, Sud'ina GF, Ullrich V. 2001. Inhibition of neutrophil spreading during adhesion to fibronectin reveals formation of long tubulovesicular cell extensions (cytonemes). Exp Cell Res 266:222–228.

Gerhardt H, Golding M, Fruttiger M, Ruhrberg C, Lundkvist A, Abramsson A, Jeltsch M, Mitchell C, Alitalo K, Shima D, Betsholtz C. 2003. VEGF guides angiogenic sprouting utilizing endothelial tip cell filopodia. J Cell Biol 161:1163–1177.

Gimsa U, Oren A, Pandiyan P, Teichmann D, Bechmann I, Nitsch R, Brunner-Weinzierl MC. 2004. Astrocytes protect the CNS: antigen-specific T helper cell responses are inhibited by astrocyte-induced upregulation of CTLA-4 (CD152). J Mol Med 82:364–372.

Grosche J, Matyash V, Moller T, Verkhratsky A, Reichenbach A, Kettenmann H. 1999. Microdomains for neuron-glia interaction: parallel fiber signaling to Bergmann glial cells. Nat Neurosci 2:139–143.

Gupta N, DeFranco AL. 2003. Visualizing lipid raft dynamics and early signaling events during antigen receptor-mediated B-lymphocyte activation. Mol Biol Cell 14:432–444.

Gustafson T, Wolpert L. 1961. Studies on the cellular basis of morphogenesis in the sea urchin embryo. Directed movements of primary mesenchyme cells in normal and vegetalized larvae. Exp Cell Res 24:64–79.

Hägerstrand H, Mrowczynska L, Salzer R, Prohaska R, Michelsen KA, Kralj-Iglič V, Iglič A. 2006. Curvature dependent lateral distribution of raft markers in the human erythrocyte membrane. Mol Membr Biol 23:277–288.

Hansson E, Ronnback L. 1995. Astrocytes in glutamate neurotransmission. FASEB J 9:343–350.

Hill TL. 1986. An introduction to statistical thermodynamics. New York: Dover Publications.

Hirrlinger J, Hulsmann S, Kirchhoff F. 2004. Astroglial processes show spontaneous motility at active synaptic terminals in situ. Eur J Neurosci 20:2235–2239.

Iglič A, Babnik B, Gimsa U, Kralj-Iglič V. 2005. On the role of membrane anisotropy in the beading transition of undulated tubular membrane structures. J Phys A Math Gen 38:8527–8536.

Iglič A, Fosnaric M, Hägerstrand H, Kralj-Iglič V. 2004. Coupling between vesicle shape and the non-homogeneous lateral distribution of membrane constituents in Golgi bodies. FEBS Lett 574:9–12.

Iglič A, Hägerstrand H. 1999. Amphiphile-induced spherical microexovesicle corresponds to an extreme local area difference

between two monolayers of the membrane bilayer. Med Biol Eng Comput 37:125–129.

Iglič A, Hägerstrand H, Bobrowska-Hägerstrand M, Arrigler V, Kralj-Iglič V. 2003. Possible role of phospholipid nanotubes in directed transport of membrane vesicles. Phys Lett A 310:493–497.

Iglič A, Hägerstrand H, Veranic P, Plemenitas A, Kralj-Iglič V. 2006. Curvature-induced accumulation of anisotropic membrane components and raft formation in cylindrical membrane protrusions. J Theor Biol 240:368–373.

Israelachvili JN. 1997. Intermolecular and surface forces. London: Academic Press.

Jahn R, Lang T, Sudhof TC. 2003. Membrane fusion. Cell 112:519–533.

Karlsson A, Karlsson R, Karlsson M, Cans AS, Stromberg A, Ryttsen F, Orwar O. 2001. Networks of nanotubes and containers. Nature 409:150–152.

Karlsson M, Sott K, Davidson M, Cans AS, Linderholm P, Chiu D, Orwar O. 2002. Formation of geometrically complex lipid nanotube-vesicle networks of higher-order topologies. Proc Natl Acad Sci USA 99:11573–11578.

Kralj-Iglič V, Hägerstrand H, Veranic P, Jezernik K, Babnik B, Gauger DR, Iglič A. 2005. Amphiphile-induced tubular budding of the bilayer membrane. Eur Biophys J 34:1066–1070.

Kralj-Iglič V, Iglič A, Gomiscek G, Arrigler V, Hägerstrand H. 2002. Microtubes and nanotubes of phospholipid bilayer vesicles. J Phys A Math Gen 35:1533–1549.

Mathivet L, Cribier S, Devaux PF. 1996. Shape change and physical properties of giant phospholipid vesicles prepared in the presence of an AC electric field. Biophys J 70:1112–1121.

Merz AJ, Higgs HN. 2003. Listeria motility: biophysics pushes things forward. Curr Biol 13:R302–R304.

Miao L, Fourcade B, Rao M, Wortis M, Zia RKP. 1991. Equilibrium budding and vesiculation in the curvature model of fluid lipid vesicles. Phys Rev E 43:6843–6856.

Miyata H, Nishiyama S, Akashi K, Kinosita K, Jr. 1999. Protrusive growth from giant liposomes driven by actin polymerization. Proc Natl Acad Sci USA 96:2048–2053.

Morata G, Basler K. 1999. Cells in search of a signal. Nat Cell Biol 1:E60–E61.

Önfelt B, Nedvetzki S, Yanagi K, Davis DM. 2004. Cutting edge: membrane nanotubes connect immune cells. J Immunol 173:1511–1513.

Ramirez-Weber FA, Kornberg TB. 1999. Cytonemes: cellular processes that project to the principal signaling center in Drosophila imaginal discs. Cell 97:599–607.

Ridet JL, Malhotra SK, Privat A, Gage FH. 1997. Reactive astrocytes: cellular and molecular cues to biological function. Trends Neurosci 20:570–577.

Robbins JR, Barth AI, Marquis H, de Hostos EL, Nelson WJ, Theriot JA. 1999. Listeria monocytogenes exploits normal host cell processes to spread from cell to cell. J Cell Biol 146:1333–1350.

Roper K, Corbeil D, Huttner WB. 2000. Retention of prominin in microvilli reveals distinct cholesterol-based lipid micro-domains in the apical plasma membrane. Nat Cell Biol 2:582–592.

Roux A, Cappello G, Cartaud J, Prost J, Goud B, Bassereau P. 2002. A minimal system allowing tubulation with molecular motors pulling on giant liposomes. Proc Natl Acad Sci USA 99:5394–5399.

Roux A, Cuvelier D, Nassoy P, Prost J, Bassereau P, Goud B. 2005. Role of curvature and phase transition in lipid sorting and fission of membrane tubules. EMBO J 24:1537–1545.

Rustom A, Saffrich R, Markovic I, Walther P, Gerdes HH. 2004. Nanotubular highways for intercellular organelle transport. Science 303:1007–1010.

Sackmann E. 1994. The seventh Datta Lecture. Membrane bending energy concept of vesicle- and cell-shapes and shape-transitions. FEBS Lett 346:3–16.

Schönenberger C, van der Zande BMI, Fokkink LGJ, Henny M, Schmid C, Krüger M, Bachtold A, Huber R, Birk H, Staufer U. 1997. Template synthesis of nanowires in porous polycarbonate membranes: electrochemistry and morphology. J Phys Chem B 101:4597–5505.

Singer SJ, Nicolson GL. 1972. The fluid mosaic model of the structure of cell membranes. Science 175:720–731.

Spees JL, Olson SD, Whitney MJ, Prockop DJ. 2006. Mitochondrial transfer between cells can rescue aerobic respiration. Proc Natl Acad Sci USA 103:1283–1288.

Sprong H, van der SP, van Meer G. 2001. How proteins move lipids and lipids move proteins. Nat Rev Mol Cell Biol 2:504–513.

Sun M, Graham JS, Hegedus B, Marga F, Zhang Y, Forgacs G, Grandbois M. 2005. Multiple membrane tethers probed by atomic force microscopy. Biophys J 89:4320–4329.

Tsafrir I, Caspi Y, Guedeau-Boudeville MA, Arzi T, Stavans J. 2003. Budding and tubulation in highly oblate vesicles by anchored amphiphilic molecules. Phys Rev Letters 9113:8102.

Turner AM, Dowell N, Turner SW, Kam L, Isaacson M, Turner JN, Craighead HG, Shain W. 2000. Attachment of astroglial cells to microfabricated pillar arrays of different geometries. J Biomed Mater Res 51:430–441.

Ventura R, Harris KM. 1999. Three-dimensional relationships between hippocampal synapses and astrocytes. J Neurosci 19:6897–6906.

Verkhratsky A, Orkand RK, Kettenmann H. 1998. Glial calcium: homeostasis and signaling function. Physiol Rev 78:99–141.

Walz W. 2000. Role of astrocytes in the clearance of excess extracellular potassium. Neurochem Int 36:291–300.

Watkins SC, Salter RD. 2005. Functional connectivity between immune cells mediated by tunneling nanotubules. Immunity 23:309–318.

Weigmann A, Corbeil D, Hellwig A, Huttner WB. 1997. Prominin, a novel microvilli-specific polytopic membrane protein of the apical surface of epithelial cells, is targeted to plasmalemmal protrusions of non-epithelial cells. Proc Natl Acad Sci USA 94:12425–12430.

Zhu AJ, Scott MP. 2004. Incredible journey: how do developmental signals travel through tissue? Genes Dev 18:2985–2997.

Zhu D, Tan KS, Zhang X, Sun AY, Sun GY, Lee JC. 2005. Hydrogen peroxide alters membrane and cytoskeleton properties and increases intercellular connections in astrocytes. J Cell Sci 118:3695–3703.

This paper was first published online on iFirst on 18 December 2006.